



# CHORUS

This is the accepted manuscript made available via CHORUS. The article has been published as:

## Super Efimov Effect of Resonantly Interacting Fermions in Two Dimensions

Yusuke Nishida, Sergej Moroz, and Dam Thanh Son

Phys. Rev. Lett. **110**, 235301 — Published 4 June 2013

DOI: [10.1103/PhysRevLett.110.235301](https://doi.org/10.1103/PhysRevLett.110.235301)

# Super Efimov effect of resonantly interacting fermions in two dimensions

Sergej Moroz,<sup>1</sup> Yusuke Nishida,<sup>2</sup> and Dam Thanh Son<sup>3</sup>

<sup>1</sup>*Department of Physics, University of Washington, Seattle, Washington 98195, USA*

<sup>2</sup>*Theoretical Division, Los Alamos National Laboratory, Los Alamos, New Mexico 87545, USA*

<sup>3</sup>*Enrico Fermi Institute, University of Chicago, Chicago, Illinois 60637, USA*

We study a system of spinless fermions in two dimensions with a short-range interaction fine-tuned to a  $p$ -wave resonance. We show that three such fermions form an infinite tower of bound states of orbital angular momentum  $\ell = \pm 1$  and their binding energies obey a universal doubly exponential scaling,  $E_3^{(n)} \propto \exp(-2e^{3\pi n/4+\theta})$ , at large  $n$ . This “super Efimov effect” is found by a renormalization group analysis and confirmed by solving the bound state problem. We also provide an indication that there are  $\ell = \pm 2$  four-body resonances associated with every three-body bound state at  $E_4^{(n)} \propto \exp(-2e^{3\pi n/4+\theta-0.188})$ . These universal few-body states may be observed in ultracold atom experiments and should be taken into account in future many-body studies of the system.

PACS numbers: 67.85.Lm, 11.10.Hi, 03.65.Ge

## Introduction

Recently topological superconductors have attracted great interest across many subfields in physics [1, 2]. This is partially because vortices in topological superconductors bind zero-energy Majorana fermions and obey non-Abelian statistics, which can be of potential use for fault-tolerance topological quantum computation [3, 4]. A canonical example of such topological superconductors is a  $p$ -wave paired state of spinless fermions in two dimensions [5], which is believed to be realized in  $\text{Sr}_2\text{RuO}_4$  [6]. Previous mean-field studies revealed that a topological quantum phase transition takes place across a  $p$ -wave Feshbach resonance [7–9].

In this Letter, we study few-body physics of spinless fermions in two dimensions right at the  $p$ -wave resonance. We predict that three such fermions form an infinite tower of bound states of orbital angular momentum  $\ell = \pm 1$  and their binding energies obey a universal doubly exponential scaling,

$$E_3^{(n)} \propto \exp(-2e^{3\pi n/4+\theta}), \quad (1)$$

at large  $n$ . Here  $\theta$  is a non-universal constant defined modulo  $3\pi/4$ . This novel phenomenon shall be termed a “super Efimov effect” because it resembles the Efimov effect in which three spinless bosons in three di-

mensions right at an  $s$ -wave resonance form an infinite tower of  $\ell = 0$  bound states whose binding energies obey the universal exponential scaling,  $E_3^{(n)} \propto e^{-2\pi n/s_0}$ , with  $s_0 \approx 1.00624$  [10] (see Table I for comparison). While the Efimov effect is possible in other situations [11, 12], it does not take place in two dimensions or with  $p$ -wave interactions [12–14]. We also provide an indication that there are  $\ell = \pm 2$  four-body resonances associated with every three-body bound state at

$$E_4^{(n)} \propto \exp(-2e^{3\pi n/4+\theta-0.188}), \quad (2)$$

which also resembles the pair of four-body resonances in the usual Efimov effect [15, 16]. These universal few-body states of resonantly interacting fermions in two dimensions should be taken into account in future many-body studies beyond the mean-field approximation.

## Renormalization group analysis

The above predictions can be derived most conveniently by a renormalization group (RG) analysis. The most general Lagrangian density that includes up to marginal couplings consistent with rotation and parity symmetries is

$$\begin{aligned} \mathcal{L} = & \psi^\dagger \left( i\partial_t + \frac{\nabla^2}{2} \right) \psi + \phi_a^\dagger \left( i\partial_t + \frac{\nabla^2}{4} - \varepsilon_0 \right) \phi_a \\ & + g \phi_a^\dagger \psi (-i\nabla_a) \psi + g \psi^\dagger (-i\nabla_{-a}) \psi^\dagger \phi_a \\ & + v_3 \psi^\dagger \phi_a^\dagger \phi_a \psi + v_4 \phi_a^\dagger \phi_{-a}^\dagger \phi_{-a} \phi_a + v'_4 \phi_a^\dagger \phi_a^\dagger \phi_a \phi_a. \end{aligned} \quad (3)$$

Here and below,  $\hbar = m = 1$ ,  $\nabla_\pm \equiv \nabla_x \pm i\nabla_y$ , and sums over repeated indices  $a = \pm$  are assumed.  $\psi$  and  $\phi_\pm$  fields correspond to spinless fermion and  $\ell = \pm 1$  composite boson, respectively. The  $p$ -wave resonance is defined by the divergence of the two-fermion scattering amplitude at zero energy, which is achieved by tuning the bare

TABLE I. Comparison between the Efimov effect versus the super Efimov effect.

Efimov effect	super Efimov effect
three bosons	three fermions
three dimensions	two dimensions
$s$ -wave resonance	$p$ -wave resonance
$\ell = 0$	$\ell = \pm 1$
exponential scaling	doubly exponential scaling



FIG. 1. Self-energy diagram of  $\phi_a$  field. Solid and dashed lines represent propagators of  $\psi$  and  $\phi_a$  fields, respectively.

detuning parameter at  $\varepsilon_0 = g^2\Lambda^2/(2\pi)$  with  $\Lambda$  being a momentum cutoff.

Since the other couplings ( $g, v_3, v_4, v'_4$ ) are all dimensionless, our effective field theory (3) is renormalizable and its renormalization can be performed in a similar way to Ref. [17]. The self-energy diagram of  $\phi_a$  field depicted in Fig. 1 is logarithmically divergent and renormalizes the two-body coupling  $g$ . The RG equation that governs the running of  $g$  at a momentum scale  $e^{-s}\Lambda$  is found to be

$$\frac{dg}{ds} = -\frac{g^3}{2\pi}, \quad (4)$$

which is solved by

$$g^2(s) = \frac{1}{\frac{s}{\pi} + \frac{1}{g^2(0)}}. \quad (5)$$

Accordingly, the two-body coupling is marginally irrelevant, i.e., it gets weak toward the infrared limit  $s \rightarrow \infty$ .

We now turn to the renormalization of the three-body coupling  $v_3$ . Diagrams that renormalize  $v_3$  are depicted in Fig. 2. By taking into account the contribution from the  $\phi_a$  field renormalization, the RG equation that governs the running of  $v_3$  is found to be

$$\frac{dv_3}{ds} = \frac{16g^4}{3\pi} - \frac{11g^2v_3}{3\pi} + \frac{2v_3^2}{3\pi}. \quad (6)$$

In the infrared limit  $s \rightarrow \infty$  where the two-body coupling scales as  $g^2 \rightarrow \pi/s$  [18], the analytic solution to Eq. (6) becomes

$$v_3(s) \rightarrow \frac{2\pi}{s} \left[ 1 - \cot\left(\frac{4}{3}(\ln s - \theta)\right) \right], \quad (7)$$

where the angle  $\theta$  depends on the initial conditions of  $g$  and  $v_3$  at the ultraviolet scale  $s \sim 0$ .

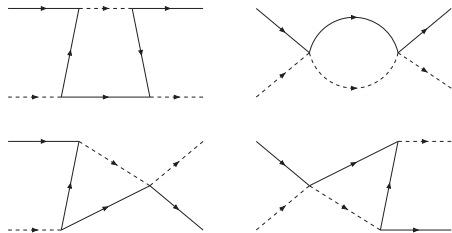


FIG. 2. Diagrams to renormalize the three-body coupling  $v_3$ .

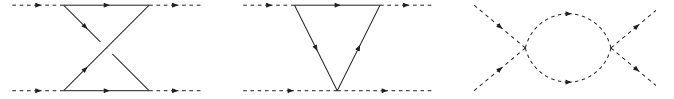


FIG. 3. Diagrams to renormalize the four-body couplings  $v_4$  and  $v'_4$ .

We find that  $sv_3$  at large  $s$  is a periodic function of  $\ln s$  and diverges at  $\ln s = 3\pi n/4 + \theta$ . These divergences in the three-body coupling indicate the existence of an infinite tower of energy scales in the three-body system in the  $\ell = \pm 1$  channels. Following the usual Efimov effect [19], we identify these scales with binding energies which leads to the prediction presented in Eq. (1). This identification will be confirmed later by solving the bound state problem.

Similarly, the four-body couplings  $v_4$  and  $v'_4$  are renormalized by diagrams depicted in Fig. 3. By taking into account the contribution from the  $\phi_a$  field renormalization, the RG equations that govern the running of  $v_4$  and  $v'_4$  are found to be

$$\frac{dv_4}{ds} = -\frac{8g^4}{\pi} + \frac{2g^2v_3}{\pi} - \frac{2g^2v_4}{\pi} + \frac{2v_4^2}{\pi} \quad (8a)$$

$$\frac{dv'_4}{ds} = -\frac{4g^4}{\pi} + \frac{2g^2v_3}{\pi} - \frac{2g^2v'_4}{\pi} + \frac{2v'^2_4}{\pi}, \quad (8b)$$

respectively. Numerical solutions to these RG equations are shown in Fig. 4 and both  $sv_4$  and  $sv'_4$  at large  $s$  are periodic functions of  $\ln s$  with period  $3\pi/4$ . We find that  $v_4$  corresponding to the  $\ell = 0$  channel diverges only at the

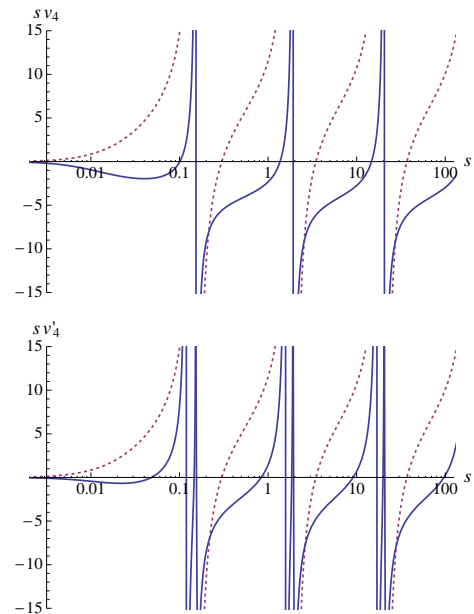


FIG. 4. RG evolutions of  $sv_4$ ,  $sv'_4$  (solid curves) and  $sv_3$  (dotted curve) with initial conditions  $g(0) = 10$ ,  $v_3(0) = i10^{-6}$ ,  $v_4(0) = v'_4(0) = 0$  [21].

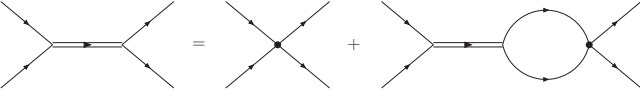


FIG. 5. Two-fermion scattering with the amplitude represented by the double line.

same points as  $v_3$ . On the other hand,  $v'_4$  corresponding to the  $\ell = \pm 2$  channels has an additional divergence at  $\ln s = 3\pi n/4 + \theta - 0.188$  associated with every point where  $v_3$  diverges. Following the RG study of spinless bosons in three dimensions [20], we identify these additional divergences with four-body resonances. We checked that this result is independent of the choice of initial conditions which leads to the prediction presented in Eq. (2).

### Bound state problem

The above predictions derived by the RG analysis can be confirmed by solving bound state problems. We employ a model Hamiltonian

$$H = \int \frac{d\mathbf{k}}{(2\pi)^2} \frac{\mathbf{k}^2}{2} \psi_{\mathbf{k}}^\dagger \psi_{\mathbf{k}} - v_0 \sum_{a=\pm} \int \frac{d\mathbf{k}d\mathbf{p}d\mathbf{q}}{(2\pi)^6} \times \chi_a(\mathbf{p}) \chi_{-a}(\mathbf{q}) \psi_{\frac{\mathbf{k}}{2}+\mathbf{p}}^\dagger \psi_{\frac{\mathbf{k}}{2}-\mathbf{p}}^\dagger \psi_{\frac{\mathbf{k}}{2}-\mathbf{q}} \psi_{\frac{\mathbf{k}}{2}+\mathbf{q}}, \quad (9)$$

which describes spinless fermions interacting by a separable  $p$ -wave potential. The form factor

$$\chi_a(\mathbf{p}) = p_a e^{-\mathbf{p}^2/(2\Lambda^2)} \quad (10)$$

is introduced to regularize the ultraviolet behavior. By summing diagrams depicted in Fig. 5, the two-fermion scattering  $T$ -matrix with incoming  $\mathbf{q}$  and outgoing  $\mathbf{p}$  relative momenta is obtained as

$$T(E; \mathbf{p}, \mathbf{q}) = \frac{16\pi |\mathbf{p}| |\mathbf{q}| \cos(\varphi_{\mathbf{p}} - \varphi_{\mathbf{q}}) e^{-(\mathbf{p}^2 + \mathbf{q}^2)/(2\Lambda^2)}}{\frac{2\pi}{v_0} - \Lambda^2 - E e^{-E/\Lambda^2} \text{E}_1(-E/\Lambda^2)}, \quad (11)$$

where  $E = \omega - \mathbf{k}^2/4 + i0^+$  is the total energy in the center-of-mass frame and  $\text{E}_1(w) \equiv \int_w^\infty dt e^{-t}/t$  is the exponential integral. Accordingly, the  $p$ -wave resonance is achieved by tuning the bare two-body coupling at  $v_0 = 2\pi/\Lambda^2$ .

A three-fermion scattering problem can be solved in a similar way to the corresponding problem in three dimensions [22, 23]. The  $T$ -matrix elements satisfy coupled integral equations depicted in Fig. 6. When the total energy approaches a binding energy  $E \rightarrow -\kappa^2 < 0$ , the  $T$ -matrix factorizes as  $T_{ab}(E; \mathbf{p}, \mathbf{q}) \rightarrow Z_a(\mathbf{p}) Z_b^*(\mathbf{q})/(E + \kappa^2)$

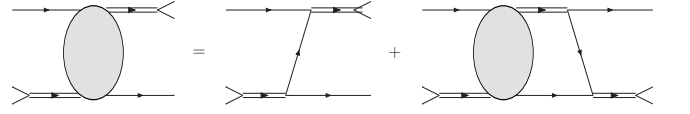


FIG. 6. Three-fermion scattering with the amplitude represented by the bulb.

and the resulting residue function satisfies

$$Z_a(\mathbf{p}) = - \int \frac{d\mathbf{q}}{2\pi} \frac{(\mathbf{p} + 2\mathbf{q})_{-a} e^{-(5\mathbf{p}^2 + 5\mathbf{q}^2 + 8\mathbf{p} \cdot \mathbf{q})/(8\Lambda^2)}}{\mathbf{p}^2 + \mathbf{q}^2 + \mathbf{p} \cdot \mathbf{q} + \kappa^2} \times \frac{\sum_{b=\pm} (2\mathbf{p} + \mathbf{q})_b Z_b(\mathbf{q})}{(\frac{3}{4}\mathbf{q}^2 + \kappa^2) e^{(\frac{3}{4}\mathbf{q}^2 + \kappa^2)/\Lambda^2} \text{E}_1((\frac{3}{4}\mathbf{q}^2 + \kappa^2)/\Lambda^2)}. \quad (12)$$

It can be seen that  $Z_+(\mathbf{p}) = e^{i(\ell-1)\varphi_{\mathbf{p}}} z_+(\mathbf{p})$  couples with  $Z_-(\mathbf{p}) = e^{i(\ell+1)\varphi_{\mathbf{p}}} z_-(\mathbf{p})$ . We focus on the  $\ell = +1$  channel in which the super Efimov effect is expected to emerge.

We first solve the two coupled integral equations (12) analytically within the leading-logarithm approximation [24]. We assume that the integral is dominated by the region where  $\kappa \ll q \ll \Lambda$  and split the integral into two parts,  $\kappa \ll q \ll p$  and  $p \ll q \ll \Lambda$ , in which a sum of  $p$  and  $q$  in the integrand is replaced with whichever is larger. This approximation simplifies Eq. (12) to

$$\frac{3}{4} z_+(p) = - \int_{\kappa}^p \frac{dq}{q} \frac{z_+(q)}{\ln \Lambda/q} - \int_p^{\epsilon \Lambda} \frac{dq}{q} \frac{z_+(q) + z_-(q)}{\ln \Lambda/q} \quad (13a)$$

$$\frac{3}{4} z_-(p) = - \int_{\kappa}^p \frac{dq}{q} \frac{z_+(q)}{\ln \Lambda/q}, \quad (13b)$$

where  $\epsilon < 1$  is a positive constant. By changing variables to  $x = \ln \ln \Lambda/p$ ,  $y = \ln \ln \Lambda/q$  and defining  $\lambda = \ln \ln \Lambda/\kappa$ ,  $\eta = \ln \ln 1/\epsilon$ , and  $\zeta_{\pm}(x) = z_{\pm}(p)$ , we obtain

$$\frac{3}{4} \zeta_+(x) = - \int_x^{\lambda} dy \zeta_+(y) - \int_{\eta}^x dy [\zeta_+(y) + \zeta_-(y)] \quad (14a)$$

$$\frac{3}{4} \zeta_-(x) = - \int_x^{\lambda} dy \zeta_+(y). \quad (14b)$$

Then the differentiation of Eqs. (14) with respect to  $x$  results in two coupled differential equations

$$\frac{3}{4} \zeta'_+(x) = -\zeta_-(x) \quad (15a)$$

$$\frac{3}{4} \zeta'_-(x) = \zeta_+(x) \quad (15b)$$

with boundary conditions

$$\frac{3}{4} \zeta_+(\eta) = - \int_{\eta}^{\lambda} dy \zeta_+(y) \quad (16a)$$

$$\frac{3}{4} \zeta_-(\lambda) = 0. \quad (16b)$$

TABLE II. Lowest six binding energies  $E_3^{(n)} = -\kappa_n^2/m$  in the form of  $\lambda_n = \ln \ln \Lambda/\kappa_n$ .

$n$	$\lambda_n$	$\lambda_n - \lambda_{n-1}$
0	0.5632	—
1	2.770	2.207
2	5.078	2.308
3	7.430	2.352
4	9.785	2.355
5	12.141	2.356
$\infty$	—	2.35619

The differential equations (15) with the boundary condition (16b) are solved by

$$\zeta_+(x) = \cos\left(\frac{4}{3}(x - \lambda)\right) \quad (17a)$$

$$\zeta_-(x) = \sin\left(\frac{4}{3}(x - \lambda)\right). \quad (17b)$$

The other boundary condition (16a) constrains the allowed value of  $\lambda$ , while we cannot determine its value within the present approximation because it is sensitive to the ultraviolet physics at  $q \sim \Lambda$ . However, owing to the periodicity of solutions (17), if  $\lambda = \theta$  is a solution, then  $\lambda = 3\pi n/4 + \theta$  must be all solutions, which is consistent with our previous RG analysis. We note that the solutions for  $\ell = -1$  are obtained simply by exchanging  $+ \leftrightarrow -$ , while the same approximation does not yield any solution for  $\ell \neq \pm 1$ . The double-logarithm scaling of solutions was also found in studying a scattering problem of three fermions [25].

We also solved the two coupled integral equations (12) with  $\ell = \pm 1$  numerically and obtained binding energies of three fermions shown in Table II. We find that they obey the universal doubly exponential scaling with period  $3\pi/4 \approx 2.35619$ , which indeed confirms our prediction in Eq. (1). While our prediction for  $\ell = \pm 2$  four-fermion resonances in Eq. (2) can be confirmed in principle in a similar way to the corresponding problem in the usual Efimov effect [15, 16], we defer this problem to a future study.

### Conclusion

In this Letter, we predicted the super Efimov effect in which resonantly interacting fermions in two dimensions form an infinite tower of  $\ell = \pm 1$  three-body bound states whose binding energies obey the universal doubly exponential scaling as in Eq. (1). We also argued that there are  $\ell = \pm 2$  four-body resonances associated with every three-body bound state as in Eq. (2). It is possible to extend our analysis away from the  $p$ -wave resonance and

draw a binding energy diagram as a function of the detuning in analogy to the usual Efimov effect [26]. These universal few-body states should be taken into account in future many-body studies of the system such as the topological quantum phase transition [5, 7]. Our super Efimov states (hopefully the lowest one) may be observed in ultracold atom experiments with  $p$ -wave Feshbach resonances [27] in the same way as the usual Efimov states through a measurement of three-body or four-body recombination atom loss [28, 29].

The authors thank Richard Schmidt for valuable discussions. This work was supported by a LANL Oppenheimer Fellowship, US DOE Grant No. DE-FG02-97ER41014, and NSF MRSEC Grant No. DMR-0820054. Part of numerical calculations was carried out at the YITP computer facility in Kyoto University.

- 
- [1] M. Z. Hasan and C. L. Kane, Rev. Mod. Phys. **82**, 3045 (2010).
  - [2] X.-L. Qi and S.-C. Zhang, Rev. Mod. Phys. **83**, 1057 (2011).
  - [3] C. Nayak, S. H. Simon, A. Stern, M. Freedman, and S. Das Sarma, Rev. Mod. Phys. **80**, 1083 (2008).
  - [4] A. Yu. Kitaev, Ann. Phys. **303**, 2 (2003).
  - [5] N. Read and D. Green, Phys. Rev. B **61**, 10267 (2000).
  - [6] A. P. Mackenzie and Y. Maeno, Rev. Mod. Phys. **75**, 657 (2003).
  - [7] V. Gurarie, L. Radzihovsky, and A. V. Andreev, Phys. Rev. Lett. **94**, 230403 (2005).
  - [8] S. S. Botelho and C. A. R. Sá de Melo, J. Low Temp. Phys. **140**, 409 (2005).
  - [9] C.-H. Cheng and S.-K. Yip, Phys. Rev. Lett. **95**, 070404 (2005).
  - [10] V. Efimov, Phys. Lett. B **33**, 563 (1970).
  - [11] V. Efimov, Nucl. Phys. A **210**, 157 (1973).
  - [12] Y. Nishida and S. Tan, Few-Body Syst. **51**, 191 (2011).
  - [13] T. K. Lim and P. A. Maurone, Phys. Rev. B **22**, 1467 (1980).
  - [14] Y. Nishida, Phys. Rev. A **86**, 012710 (2012).
  - [15] H.-W. Hammer and L. Platter, Eur. Phys. J. A **32**, 113 (2007).
  - [16] J. von Stecher, J. P. D’Incao, and C. H. Greene, Nature Phys. **5**, 417 (2009).
  - [17] Y. Nishida, Phys. Rev. D **77**, 061703(R) (2008).
  - [18] In this case, the RG equation (6) can be brought into the canonical form,  $d(sv_3)/d(\ln s) = \alpha + \beta(sv_3) + \gamma(sv_3)^2$ , where  $\alpha = 16\pi/3$ ,  $\beta = -8/3$ ,  $\gamma = 2/(3\pi)$ . The form of general solutions can be classified according to the sign of the discriminant of the right hand side. See Appendix D in S. Moroz, S. Floerchinger, R. Schmidt, and C. Wetterich, Phys. Rev. A **79**, 042705 (2009).
  - [19] P. F. Bedaque, H.-W. Hammer, and U. van Kolck, Phys. Rev. Lett. **82**, 463 (1999); Nucl. Phys. A **646**, 444 (1999).
  - [20] R. Schmidt and S. Moroz, Phys. Rev. A **81**, 052709 (2010).
  - [21] A small imaginary part is introduced in  $v_3(0)$  to facilitate the numerical evaluation in the whole domain of  $s$ . Plotted are real parts of the couplings. See discussions in

- Ref. [20].
- [22] J. Levinsen, N. R. Cooper, and V. Gurarie, *Phys. Rev. Lett.* **99**, 210402 (2007).
- [23] M. Jona-Lasinio, L. Pricoupenko, and Y. Castin, *Phys. Rev. A* **77**, 043611 (2008).
- [24] D. T. Son, *Phys. Rev. D* **59**, 094019 (1999).
- [25] J. Levinsen, N. R. Cooper, and V. Gurarie, *Phys. Rev. A* **78**, 063616 (2008).
- [26] F. Ferlino and R. Grimm, *Physics* **3**, 9 (2010).
- [27] C. Chin, R. Grimm, P. Julienne, and E. Tiesinga, *Rev. Mod. Phys.* **82**, 1225 (2010).
- [28] T. Kraemer, M. Mark, P. Waldburger, J. G. Danzl, C. Chin, B. Engeser, A. D. Lange, K. Pilch, A. Jaakkola, H.-C. Nägerl, and R. Grimm, *Nature* **440**, 315 (2006).
- [29] F. Ferlino, S. Knoop, M. Berninger, W. Harm, J. P. D’Incao, H.-C. Nägerl, and R. Grimm, *Phys. Rev. Lett.* **102**, 140401 (2009).